NREL/CP-530-22966 • UC Category: 1250

FTIR, EPMA, Auger, and XPS Analysis of Impurity Precipitates in CdS Films

J.D. Webb, D.H. Rose, D.W. Niles,
A. Swartzlander, and M.M. Al-Jassim
Presented at the 26th IEEE Photovoltaic Specialists Conference, September 29–October 3, 1997, Anaheim, California

National Renewable Energy Laboratory
1617 Cole Boulevard
Golden, Colorado 80401-3393
A national laboratory of
the U.S. Department of Energy
Managed by Midwest Research Institute
for the U.S. Department of Energy
under contract No. DE-AC36-83CH10093

Prepared under Task No. PV703101

September 1997

FTIR, EPMA, AUGER, AND XPS ANALYSIS OF IMPURITY PRECIPITATES IN CDS FILMS

John D. Webb, Doug H. Rose, David W. Niles, Amy Swartzlander, and Mowafak M. Al-Jassim
National Renewable Energy Laboratory (NREL), Golden, CO 80401-3393

ABSTRACT

Impurities in cadmium sulfide (CdS) films are a concern in the fabrication of copper (indium, gallium) diselenide (CIGS) and cadmium telluride (CdTe) photovoltaic devices. Films of CdS grown using chemical bath deposition (CBD) generally yield better devices than purer CdS films grown using vacuum deposition techniques, despite the higher impurity concentrations typically observed in the CBD CdS films. In this work, we present Fourier transform infrared (FTIR), Auger, electron microprobe (EPMA), X-ray photoelectron spectroscopic (XPS), and secondary ion mass spectroscopic (SIMS) analyses of the impurities in CBD CdS films, and show that these differ as a function of substrate type and film deposition conditions. We also show that some of these impurities exist as 10^2 micron-scale precipitates.

INTRODUCTION

Thin films of CdS play an essential role in the creation of junctions, buffers, or passivation layers in thin-film photovoltaic (PV) devices [1,2]. The best device performance has generally been achieved with solar cells incorporating CdS films grown by CBD, rather than CdS films grown using other methods, such as physical vapor deposition (PVD) [2,3]. Recently, considerable attention has focused upon the effects of components of the CBD solution on CIGS PV films [2] and upon side products of the CBD reaction. Typical CBD solutions contain a soluble cadmium salt, ammonia, and thiourea [4] and sometimes utilize triethanolamine as a complexing agent for cadmium ion [1] or an ammonium salt as a pH buffer [3]. Sebastian, *et al.* [1] have observed an impurity phase apparently consisting of cadmium cyanamide (CdNCN) in CBD CdS films on glass substrates. This phase can be removed by rinsing the CdS film in dilute acetic acid [1]. Friedlmeier, *et al.* [5] have identified 30–50 nm-wide islands containing cadmium and oxygen on CIGS surfaces during the initial stages of CBD CdS film growth, which they postulate to consist of $Cd(OH)_2$. Urea [1] and cyanamide [5] have been identified as the primary products of the CBD reaction. In a recent study, FTIR spectroscopy and XPS were used to identify hydroxyl ions (OH^-), water (H_2O), cyanamides, and carbonates in CBD CdS films on a variety of substrates (none of these species were detected in CdS films deposited by evaporation) [6].

The variety of possible products and by-products of the CBD reaction, and the potential for aqueous ammonia to act as a complexing agent for both cadmium [1,7] and copper [7] ions, suggest that minor variations in the CBD process chemistry may have a significant influence on the CdS/CIGS interface and on the performance of the resulting devices. While significant effects on CIGS absorber film properties resulting from exposure of the films to CBD solutions without thiourea have been cited recently [2], other work incorporating slightly different chemical bath recipes [3] reveals no such effects. The effect of processing parameters on the ZnO/CdS interface, and on device performance, has also been investigated [4]. We have presented Fourier transform photoluminescence (FT-PL) data which show that exposure of CIGS films to components of the CBD solutions, without deposition of CdS, increases PL intensity of the CIGS films almost as much as application of CdS films, implying that these individual components can reduce the rate of nonradiative recombination in the CIGS films [7]. In CdTe thin-film PV devices, which are grown on CdS film substrates to form an active heterojunction, the CBD process for CdS has produced high efficiencies [8], although alternatives to the CBD process, such as close-spaced sublimation, are being actively pursued [8,9]. The influence of ambient oxygen during close-spaced sublimation is also being studied [8,9]. An XPS investigation of oxygen-containing impurities in CBD CdS films on glass and InP substrates concluded that the major O-containing impurity species is water incorporated from the chemical bath [10].

EXPERIMENTAL APPROACH

Infrared spectroscopy and various surface analysis techniques have been used previously to identify chemical species on relatively large areas of CdS films [6,10]. An emerging issue in CdS film technology is to identify the chemical nature of the small nonuniformities visible under sufficient magnification on the surfaces of a variety of samples incorporating CBD CdS films. For this purpose, non-destructive FTIR microspectroscopy was used in this work in concert with micro and macro-scale surface analytical techniques. The Nicolet NicPlan FTIR microscope was operated in the reflection mode as an accessory to a Nicolet 510 FTIR spectrophotometer at a resolution of 4 cm^{-1}. The FTIR microscope can obtain infrared reflectance (R) or transmittance (T) spectra of sample areas as small as 20 x 20 µm. These areas are selected using visible light microscopy and are then analyzed using IR radiation focused through an aperture sized to encompass the area of interest. A reference spectrum is also taken, through the same aperture, of a visually defect-free area of the sample, which is ratioed into the sample spectrum to yield R or T spectra of the area of interest. The conductive substrates (SnO_2, Mo, or InP) for the CdS films examined in this work dictated use of the reflectance mode. The incident IR beam passed through the CdS film before and after reflection from the substrate. The resulting R spectra were converted to reflection-absorbance (RA = -log [1/R]) spectra for comparison with infrared spectral databases for chemical compounds, which are stored in absorbance

units. The FTIR microscope can be set to automatically scan a preset traverse or grid of the sample, record the spectra at each traverse or grid point, and prepare a two- or three-dimensional "map" of the intensity of infrared absorbance associated with a given chemical species vs. sample position. A JEOL JXA-8900L electron probe microanalysis (EPMA) system with 5-µm e-beam diameter was operated at 10 kV and 20 nA beam current to provide qualitative wavelength-dispersive scans and elemental analyses of sample regions previously scanned using the FTIR microscope. A PHI 670i field-emission scanning Auger nanoprobe, a PHI 5600 XPS system with monochromatic Al x-ray source and 0.8 mm analysis spot diameter, and a Cameca IV time-of-flight (TOF) SIMS system were also used in this work.

RESULTS AND DISCUSSION

Fig. 1 shows one of a series of FTIR-RA spectra of 50 x 50 µm areas collected near a visible anomaly on an experimental CBD CdS/CIGS/Mo PV device without a ZnO overlayer. In addition to sinusoidal interference fringes caused by multiple reflections within the partially transparent thin films comprising the device, the spectrum shows a broad -OH absorbance near 3500 cm^{-1} probably caused by sorbed water, as well as two sharp absorbances near 1650 and 1400 cm^{-1}. A micrograph of a 320 x 220 µm region of the sample showing the midpoints of the sampling locations is at upper right in Fig.1. The micrograph also shows a light-colored spot (actually orange) about 50 µm in diameter; the cross shows the location within this spot at which the spectrum shown was taken. Numerous smaller orange spots were observed visually on this sample using the FTIR microscope. At lower right in the figure is a three-dimensional "map" of the integrated RA of the shaded peak near 1400 cm^{-1} in the spectrum, derived from all 176 of the FTIR-RA spectra taken in the region of the 50-µm spot. At lower left is an infrared contour map of the same region. Both of these plots show a strong correlation between the intensity of absorbance at 1400 cm^{-1} and the location of the orange spot in the micrograph, and show that the impurity absorbances were strongest at the spot marked by the cross in the micrograph where the displayed spectrum was collected. Fig. 2 shows the same FTIR-RA spectrum displayed in Fig. 1, treated to remove the broad interference fringes and water absorbance bands. Library searches of this spectrum vs. the Sadtler Select Inorganics spectral database [11] gave absorbance spectra of bicarbonates (Fig. 2) or carbonates as likely matches to the spectrum of the orange spot. EPMA analyses show that the spot protrudes above the CdS film surface, that it contains carbon, oxygen, copper, indium, and selenium in addition to cadmium and sulfur, but not nitrogen or gallium. EPMA analyses of areas adjacent to the spot show only cadmium and sulfur.

Our interpretation of these results is that the spot contains normal or basic copper carbonate [12] resulting from a side reaction between the CIGS film (or its surface oxides and binary phases) and the CBD bath. The CBD process for this sample involved the reaction of thiourea with cadmium acetate in ammonia-buffered aqueous solution at 75°C. Copper oxides and selenides are soluble in aqueous ammonia [12], and copper selenides are present as binary phases in copper-rich CIGS films [13]. Carbonates and bicarbonates can precipitate from solutions containing CO_2 and metal ions, and CO_2 is readily evolved from heated basic solutions of acetates [14], such as the ammoniated CBD bath. An alternative route for carbonate ion formation has been postulated as a result of absorption of atmospheric CO_2 by the basic CBD solution [6]. Carbonates have been observed on the surfaces of similar devices by using large-area FTIR and XPS analyses [6]; our work indicates that the carbonates are in the form of localized precipitates on the device surfaces. Although indium was also observed in the spot, copper carbonates are the likeliest carbon-containing constituents given the solubility of copper compounds in ammonia [12], the insolubility of indium compounds in ammonia, and the lack of references to indium carbonates [15]. The indium in the spot may be present as oxides [16] or selenates, which would be consistent with the EPMA analysis but difficult to detect using FTIR microspectroscopy because of the low IR absorption frequencies of these species. The evidence for incorporated water and ionic salts in the spot analyzed, as well as its size, indicate that it could function as a shunt or initiate delamination in a finished device.

We also examined a series of 0.1-µm thick CBD CdS films on glass substrates coated with SnO_2:F/iSnO_2 [17]. These samples are typical substrates for CdTe deposition, and contained numerous visible anomalies in the form of spots 50–100 µm in diameter. The CBD process for these samples involved the reaction of thiourea with cadmium acetate in ammonia-buffered aqueous solution at 86°–87° C, followed by ultrasonic agitation and rinsing in deionized water [18]. Using FTIR microspectroscopy and searches of spectral databases [11,19], we have identified acetate, sulfate, and cyanamide ionic species in black spots visible on or in the as-deposited CBD CdS films (Fig. 3). The cyanamide ionic species (probably cadmium cyanamide) can be distinguished from cyanamide, the expected reaction product, by its lower vibrational frequency [19]. We have confirmed the presence of cadmium, nitrogen, chlorine, carbon, sulfur, and oxygen in various of these spots using the scanning Auger nanoprobe and XPS with light sputtering. Annealing the samples in hydrogen at 400°C removes the (cadmium) cyanamide IR signature but leaves the acetate IR bands intact. Similar IR results were obtained for samples subjected to dilute HCl rinses, followed by annealing at 500°C in hydrogen or at 600°C in helium. A dilute HCl rinse, followed by annealing at 600°C in oxygen, removes all of the IR-absorbing organic species from the as-deposited samples. The 500°C and 600°C anneals leave tin-rich spots on the sample surfaces, as confirmed using the Auger microprobe. The localized tin-rich spots probably result from a redox reaction between the organic impurity precipitates and the SnO_2 substrates. The failure to remove the soluble acetate precipitates through the deionized water rinse could be explained if these precipitates were encapsulated by a thin, insoluble CdS overlayer. Any of these spots, regardless of the rinsing/annealing procedure, could act as shunts or delamination sites in a finished CdTe/CdS device.

Using FTIR microspectroscopy and TOF-SIMS, we have identified cyanamides, cyanates (-O-C≡N) or thiocyanates (-S-C≡N), and sulfates ($SO_4^{=}$) in large (200-µm diameter) red precipitates visible in CBD CdS films grown on InP substrates. FTIR microspectroscopy also shows that the nitrogen-containing species are dispersed throughout the CdS films on InP, but are concentrated in the red spots.

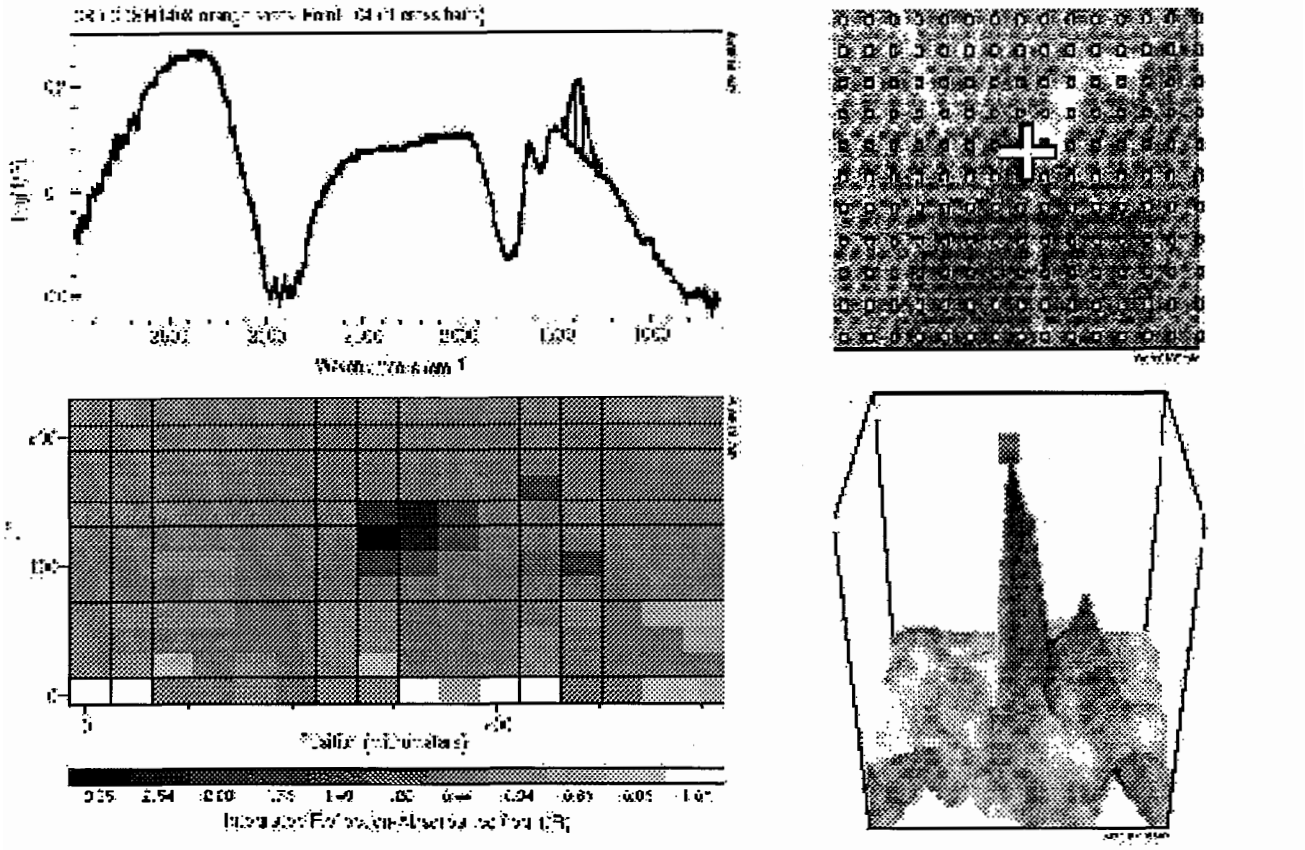

Fig. 1. FTIR microspectroscopic analysis of 50-μm orange spot on CdS/CIGS/Mo sample.

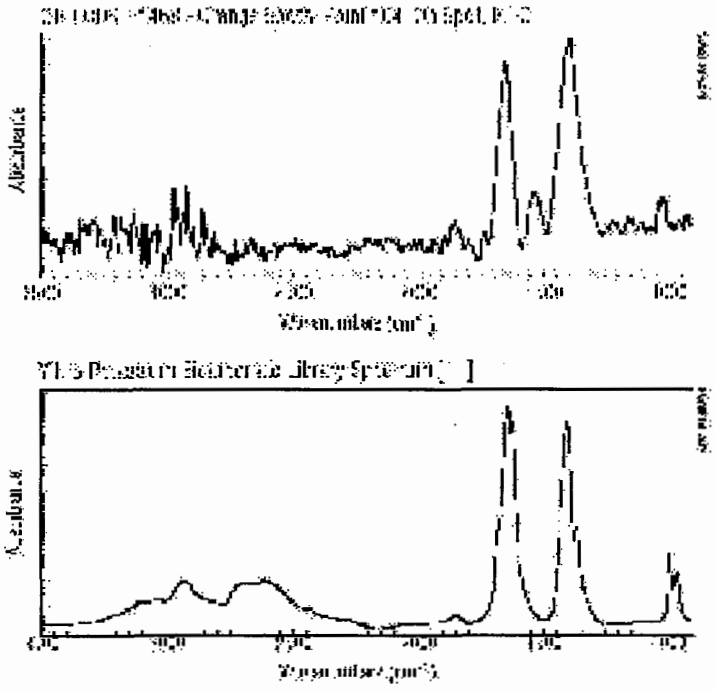

Fig. 2. Spectral database [11] search result (bottom) for fringe-corrected FTIR-RA spectrum of orange spot (top).

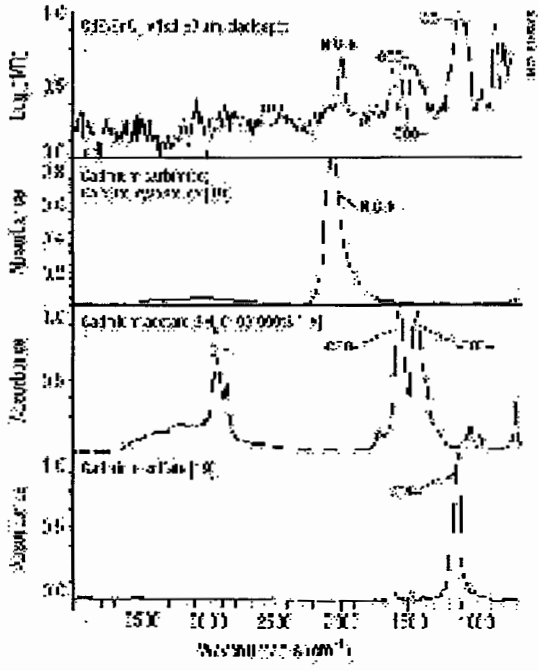

Fig. 3. FTIR microreflectance spectrum of 50-μm black spot on as-deposited CdS/SnO$_2$ sample, with library spectra [19] of probable contaminants.

CONCLUSIONS

The wide variety of chemical species observed in the CdS films is ascribed to variations in the CBD conditions and substrates. These species occur primarily as precipitates or precipitate clusters with diameters up to 200 µm. In the CdS/CIGS device, the dimensions and prevalence of the impurity-containing spots suggest that a fairly extensive reaction, requiring a significant volume fraction of soluble precursors such as CuSe or CuO, occurred between the CBD solution and the absorber film to yield carbonates. In the CdS/SnO_2 samples, post-CBD annealing treatments alter the composition of the impurity precipitates but do not remove them without leaving tin-rich spots behind. Although the CBD process for CdS yields high-quality devices in many cases, the size and extent of the precipitates observed suggest potential performance problems. Our current research efforts are being focused to determine the extent of the precipitate problem, to correlate precipitate formation with CBD conditions and substrate types, and to determine the effect of the precipitates on device performance. We infer from these preliminary results that modification of the CBD process to prevent co-deposition of impurity precipitates in the CdS films, rather than post-CBD treatments, will prove most effective in producing clean, uniform CdS films. FTIR microspectroscopy, in conjunction with surface analysis, is a key component of this effort.

ACKNOWLEDGMENTS

The authors acknowledge the contributions of Jay Riker, Sally Asher, and Alice Mason of NREL for providing the CdS/InP samples and providing TOF-SIMS and EPMA analyses, respectively. We also thank Jeff Britt of Energy Photovoltaics (Lawrenceville, NJ 08648) and Andrew Gabor (Evergreen Solar, Waltham, MA 02154) for providing the CdS/CIGS sample. This work was performed under U.S. Department of Energy contract number DE-AC36-83CH10093.

REFERENCES

1. P.J. Sebastian, J. Campos, and P.K. Nair, *Thin Solid Films* **227**, pp. 190-195 (1993).
2. K. Zweibel, H.S. Ullal, and B. von Roedern, "Progress and Issues in Thin-Film PV Technologies," 25th IEEEPhotovoltaic Specialists Conference, 1996, pp. 745-750.
3. S. Li Sheng, B.J. Stanbery, C.H. Huang, C.H. Chang, Y.S. Chang, and T.J. Anderson, "Effects of Buffer Layer Processing on CIGS Excess Carrier Lifetime," 25th IEEE PVSC, 1996, pp. 821-824.
4. K. Ramanathan, M.A. Contreras, J.R. Tuttle, J. Keane, J.D. Webb, S. Asher, D. Niles, R. Dhere, A.L. Tennant, F.L. Hasoon, and R. Noufi, "Effect of Heat Treatments and Window Layer Processing on the Characteristics of $CuInGaSe_2$ Thin Film Solar Cells," 25th IEEE PVSC, 1996, pp. 837-840.
5. T.M. Friedlmeier, D. Braunger, D. Hariskos, M. Kaiser, H.N. Wanka, and H.W. Schock, "Nucleation and Growth of the CdS Buffer Layer on $Cu(In,Ga)Se_2$ Thin Films," 25th IEEE PVSC, 1996, pp. 845-848.
6. A. Kylner, A. Rockett, and L. Stolt, "Oxygen in Solution-Grown CdS Films for Thin Film Solar Cells," *Solid State Phenomena* **51-52**, pp. 533-540 (1996).
7. J.D. Webb, B.M. Keyes, K. Ramanathan, P. Dippo, D.W. Niles, and R. Noufi, "FT-PL Analysis of CIGS/CdS/ZnO Interfaces," Proc. DOE/NREL Photovoltaic Program Review, Lakewood, CO, 1996, pp. 573-578.
8. C.S. Ferekides, D. Marinskiy, B. Marinskaya, B. Tetali, D. Oman, and D.L. Morel, "CdS Films Prepared by the Close-Spaced Sublimation and Their Influence on CdTe/CdS Solar Cell Performance," 25th IEEE PVSC, 1996, pp. 751-756.
9. D.H. Rose, D.H. Levi, R.J. Matson, D.S. Albin, R.G. Dhere, and P. Sheldon, "The Role of Oxygen in CdS/CdTe Solar Cells Deposited by Close-Spaced Sublimation," 25th IEEE PVSC, 1996, pp. 777-780.
10. D. W. Niles, G Herdt, and M. Al-Jassim, "An X-Ray Photoelectron Spectroscopy Investigation of O Impurity Chemistry in CdS Thin Films Grown by Chemical Bath Deposition," *J. Appl. Phys.* **81**, 4, 1978-1994 (1997).
11. Sadtler Div., Bio-Rad Laboratories, Philadelphia, PA 19104. The digital library contains the mid-IR spectra of 1300 inorganic chemicals. The accompanying IR Searchmaster software contains various correlation algorithms for comparing the spectra of unknown samples to the library spectra.
12. D.R. Lide, ed., *CRC Handbook of Chemistry and Physics*, 75th ed., CRC Press, Boca Raton, Fla., pp. 4-56-4-58.
13. J.R. Tuttle, M. Contreras, A. Tennant, D. Albin, and R. Noufi, "High-Efficiency Thin-Film $Cu(In, Ga)Se_2$-Based Photovoltaic Devices: Progress Towards A Universal Approach to Absorber Fabrication," 23rd IEEE PVSC, 1993, pp. 415-421.
14. J. Marsh, *Advanced Organic Chemistry*, 2nd ed., Mc-Graw-Hill, New York, p. 569 (1977).
15. Ibid 12, p. 4-63.
16. M.E. Boiko and G.A. Medvedkin, "Thermal Oxidation of $CuInSe_2$: Experiment and Physico-Chemical Model," 24th IEEE PVSC, 1994, pp. 258 - 261.
17. D. Albin, D. Rose, R. Dhere, D. Niles, A. Swartzlander, A. Mason, D. Levi, H. Moutinho, and P. Sheldon, "Tin Oxide Stability Effects," Proc. DOE/NREL Photovoltaic Program Review, Lakewood, CO, 1996, pp. 665-681.
18. D.H. Rose, D.S. Albin, R.J. Matson, A.B. Swartzlander, X. S. Li, R.G. Dhere, S. Asher, F.S. Hasoon, and P. Sheldon, "Effects of Oxygen During Close-Spaced Sublimation of CdTe Solar Cells," Proc MRS **426**, 1996, pp. 337-348.
19. Nicolet Instrument Corp., Madison, WI 53711. The complete Nicolet digital library contains the mid-IR spectra of appr. 50,000 compounds (mostly organics), and includes various correlation algorithms for comparing the spectra of unknown samples to the library spectra.